

A Monte Carlo Rendering Framework for Simulating Optical Heterodyne Detection - Supplementary Material

JUHYEON KIM, Dartmouth College, USA

CRAIG BENKO, MAGNUS WRENNINGE, RYUSUKE VILLEMEN, and ZEB BARBER, Aurora Innovation, USA

WOJCIECH JAROSZ and ADITHYA PEDIREDLA, Dartmouth College, USA

CCS Concepts: • Computing methodologies → Ray tracing; Computational photography.

Additional Key Words and Phrases: optical interferometry, Doppler effect, time-of-flight rendering, physically-based rendering, computational imaging

ACM Reference Format:

Juhyeon Kim, Craig Benko, Magnus Wrenninge, Ryusuke Villemien, Zeb Barber, Wojciech Jarosz, and Adithya Pediredla. 2025. A Monte Carlo Rendering Framework for Simulating Optical Heterodyne Detection - Supplementary Material. *ACM Trans. Graph.* 44, 4 (August 2025), 4 pages. <https://doi.org/10.1145/3731150>

1 PATH VELOCITY DERIVATION

We first derive the derivative relationship between path length and path velocity. For recall, we defined the (optical) path velocity $u(\bar{x})$ as

$$u(\bar{x}) = \sum_{k=0}^{K-1} \eta_k (\mathbf{v}_k - \mathbf{v}_{k+1}) \cdot \hat{\mathbf{d}}_k \quad (1)$$

and (optical) path length $l(\bar{x})$ as follow

$$l(\bar{x}) = \sum_{k=0}^{K-1} \eta_k \|\mathbf{x}_{k+1} - \mathbf{x}_k\|. \quad (2)$$

Note that \mathbf{x}_k are all functions of time t , but we omitted them for brevity.

As Fig. 1-(B), we can calculate distance change for path segment $\|\mathbf{x}_{k+1} - \mathbf{x}_k\|$ after the infinitesimal time change of Δt .

$$\begin{aligned} \|\mathbf{x}_{k+1} + \mathbf{v}_{k+1}\Delta t - \mathbf{x}_k - \mathbf{v}_k\Delta t\|^2 &= \|\mathbf{x}_{k+1} - \mathbf{x}_k\|^2 \\ &+ 2(\mathbf{x}_{k+1} - \mathbf{x}_k) \cdot (\mathbf{v}_{k+1} - \mathbf{v}_k)\Delta t + \|\mathbf{v}_{k+1} - \mathbf{v}_k\|^2\Delta t^2 \end{aligned} \quad (3)$$

Authors' addresses: Juhyeon Kim, Dartmouth College, USA, juhyeon.kim.gr@dartmouth.edu; Craig Benko, cbenko@aurora.tech; Magnus Wrenninge, mwrenninge@aurora.tech; Ryusuke Villemien, rvillemien@aurora.tech; Zeb Barber, zbarber@aurora.tech; Aurora Innovation, USA; Wojciech Jarosz, wojciech.k.jarosz@dartmouth.edu; Adithya Pediredla, adithya.k.pediredla@dartmouth.edu, Dartmouth College, USA.

Permission to make digital or hard copies of all or part of this work for personal or classroom use is granted without fee provided that copies are not made or distributed for profit or commercial advantage and that copies bear this notice and the full citation on the first page. Copyrights for components of this work owned by others than the author(s) must be honored. Abstracting with credit is permitted. To copy otherwise, or republish, to post on servers or to redistribute to lists, requires prior specific permission and/or a fee. Request permissions from permissions@acm.org.

© 2025 Copyright held by the owner/author(s). Publication rights licensed to ACM. 0730-0301/2025/8-ART \$15.00

<https://doi.org/10.1145/3731150>

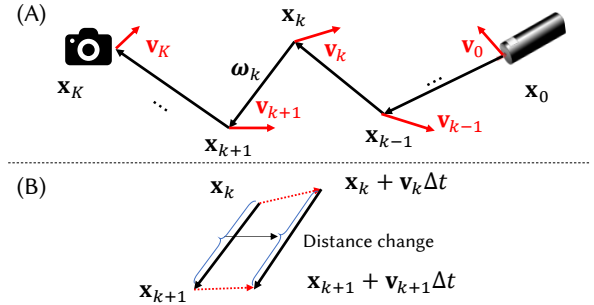


Fig. 1. (A) Time evolving path consist of $K + 1$ vertices and its instantaneous velocity. (B) By calculating distance change after infinitesimal time Δt , we can also derive path velocity.

Ignoring the Δt^2 term and taking square-root gives:

$$\begin{aligned} &\|\mathbf{x}_{k+1} + \mathbf{v}_{k+1}\Delta t - \mathbf{x}_k - \mathbf{v}_k\Delta t\| \\ &= \|\mathbf{x}_{k+1} - \mathbf{x}_k\| \left(1 + \frac{2(\mathbf{x}_{k+1} - \mathbf{x}_k) \cdot (\mathbf{v}_{k+1} - \mathbf{v}_k)\Delta t}{\|\mathbf{x}_{k+1} - \mathbf{x}_k\|^2} \right)^{1/2} \\ &\approx \|\mathbf{x}_{k+1} - \mathbf{x}_k\| \left(1 + \frac{(\mathbf{x}_{k+1} - \mathbf{x}_k) \cdot (\mathbf{v}_{k+1} - \mathbf{v}_k)\Delta t}{\|\mathbf{x}_{k+1} - \mathbf{x}_k\|^2} \right) \\ &= \|\mathbf{x}_{k+1} - \mathbf{x}_k\| + \frac{\mathbf{x}_{k+1} - \mathbf{x}_k}{\|\mathbf{x}_{k+1} - \mathbf{x}_k\|} \cdot (\mathbf{v}_{k+1} - \mathbf{v}_k)\Delta t \\ &= \|\mathbf{x}_{k+1} - \mathbf{x}_k\| + \hat{\mathbf{d}}_k \cdot (\mathbf{v}_{k+1} - \mathbf{v}_k)\Delta t \end{aligned} \quad (4)$$

Therefore,

$$\frac{d}{dt} \|\mathbf{x}_{k+1} - \mathbf{x}_k\| = \hat{\mathbf{d}}_k \cdot (\mathbf{v}_{k+1} - \mathbf{v}_k). \quad (5)$$

Multiplying η_k and summing up for all path segments gives

$$u(\bar{x}) = -\frac{d}{dt} l(\bar{x}), \quad (6)$$

which completes the proof. Considering that the Doppler effect arises from infinitesimal distance change, it is intuitively understandable that $u(\bar{x}) = -\frac{d}{dt} l(\bar{x})$.

2 DISCUSSION ON HETERODYNE EFFICIENCY

2.1 Nature of Heterodyne Efficiency

Heterodyne efficiency η_h is defined as:

$$\eta_h = \frac{\langle |i_{AC}|^2 \rangle}{\langle i_{LO} \rangle \langle i_s \rangle} = \frac{\int_{\mathcal{A}_{det}^2} \Gamma_s(\vec{r}_1, \vec{r}_2) \Gamma_{LO}^*(\vec{r}_1, \vec{r}_2) d\vec{r}_1 d\vec{r}_2}{\left(\int_{\mathcal{A}_{det}} \Gamma_{LO}(\vec{r}, \vec{r}) d\vec{r} \right) \left(\int_{\mathcal{A}_{det}} \Gamma_s(\vec{r}, \vec{r}) d\vec{r} \right)}, \quad (7)$$

where i_{LO} and i_s are photocurrent from the local oscillator and incident field only, respectively. The primary advantage of introducing heterodyne efficiency is that it allows us to express the photocurrent

power as a product of the radiometric powers from the local oscillator and the incident field, scaled by the attenuation constant η_h . In this work, our focus is on the distribution of the photocurrent in the spectral domain, rather than the absolute scale (or normalization factor) of the distribution, which is determined by the heterodyne efficiency. Thus, we assume that η_h is given and constant over the measurement time. Additionally, we assume η_h is constant over the frequency range of interest, as frequency shifts due to Doppler effects or chirps are negligible compared to the carrier frequency.

While we do not delve into the detailed evaluation of heterodyne efficiency, it is generally expressed as:

$$\eta_h = \frac{1}{N_{\text{speckle}}} = \frac{\mathcal{A}_{\text{coh}}}{\mathcal{A}_{\text{det}}} \quad (8)$$

where N_{speckle} denotes the number of independent speckle grains on the photodetector, and \mathcal{A}_{coh} represents the coherence area (or speckle grain size) [Cummins and Swinney 1970; Goodman 2007]. We can intuitively understand this since $\Gamma_s(\vec{r}_1, \vec{r}_2)$ becomes zero if \vec{r}_1 and \vec{r}_2 belong to different speckle grains, which are mutually incoherent. Therefore, only the single speckle grain can effectively contribute to heterodyne power. Readers interested in a precise evaluation of heterodyne efficiency are referred to Fried [1967]; Yura [1974].

2.2 Assumption of Constant Optical Spectrum

In the main manuscript, we assume that the optical spectrum is approximately constant over the detector to exploit heterodyne efficiency. Such assumption allows the mutual coherence function to be decomposed into spatial and temporal components [Steinberg and Yan 2021]:

$$\Gamma_s(\vec{r}_1, \vec{r}_2, \tau) = \Gamma_s(\vec{r}_1, \vec{r}_2) \tilde{\Gamma}_s(\tau) \quad (9)$$

where $\tilde{\Gamma}_s$ is the normalized temporal term, ensuring that the magnitude is preserved. Note that this constant-spectrum assumption is much more reasonable compared to the constant-phase assumption which denies the existence of speckles. This constant-spectrum assumption may fail if the detector size (typically 10 μm -1 mm scale) is large compared to the object distance (typically in 30 cm-100 m scale), which is generally not the case. Using this assumption, the autocorrelation function becomes:

$$C_{AC}(\tau) = \tilde{\Gamma}_s(\tau) \tilde{\Gamma}_{LO}^*(\tau) \int_{\mathcal{A}_{\text{det}}} \Gamma_s(\vec{r}_1, \vec{r}_2) \Gamma_{LO}^*(\vec{r}_1, \vec{r}_2) d\vec{r}_1 d\vec{r}_2. \quad (10)$$

Applying the definition of heterodyne efficiency, this simplifies to:

$$C_{AC}(\tau) = \eta_h \tilde{\Gamma}_s(\tau) \tilde{\Gamma}_{LO}^*(\tau) \left(\int_{\mathcal{A}_{\text{det}}} \Gamma_s(\vec{r}, \vec{r}) d\vec{r} \right) \left(\int_{\mathcal{A}_{\text{det}}} \Gamma_{LO}^*(\vec{r}, \vec{r}) d\vec{r} \right). \quad (11)$$

Since $\Gamma_s(\vec{r}, \vec{r}, \tau) = \Gamma_s(\vec{r}, \vec{r}) \tilde{\Gamma}_s(\tau)$, we have

$$C_{AC}(\tau) = \eta_h \left(\int_{\mathcal{A}_{\text{det}}} \Gamma_s(\vec{r}, \vec{r}, \tau) d\vec{r} \right) \left(\int_{\mathcal{A}_{\text{det}}} \Gamma_{LO}^*(\vec{r}, \vec{r}, \tau) d\vec{r} \right). \quad (12)$$

Taking the Fourier transform of the above equation yields:

$$S_{AC}(\omega) = \eta_h \mathcal{A}_{\text{det}}^2 S_S(\omega) * S_{LO}^*(-\omega), \quad (13)$$

where $S_{LO}(\omega)$ and $S_S(\omega)$ represent the *optical spectra* of the LO and the incident field, which were assumed to be constant over the detector.

3 PROOF OF CONDITIONS FOR STATIONARY $i_{AC}(t)$

Here, we show if and only if the condition that $i_{AC}(t)$ becomes stationary is $\phi_{LO}(t)$ is linear or quadratic with regard to t . Recall that $i_{AC}(t)$ is represented as

$$i_{AC}(t) = E_{LO}(t) E_s^*(t). \quad (14)$$

Let's define d as the ToF term. E_s is assumed to be a stochastic process which is represented as

$$E_s(t) = A e^{j\psi} e^{j\phi_s(t)} \quad (15)$$

where we also assume A, ψ are t independent random variables. We have the following autocorrelation form,

$$\begin{aligned} \langle i_{AC}(t) i_{AC}^*(t + \tau) \rangle &= \langle E_{LO}(t) E_{LO}^*(t - d) E_{LO}^*(t + \tau) E_{LO}(t - d + \tau) \rangle \\ &= A_{LO}^2 \langle |A|^2 \rangle e^{j(\phi_{LO}(t) - \phi_{LO}(t + \tau) - \phi_s(t) + \phi_s(t + \tau))} \end{aligned} \quad (16)$$

Ignoring Doppler frequency shift for simplicity, we can represent ϕ_s as $\phi_{LO}(t - d)$, where d is ToF. We will drop LO from now for simplicity. Also, we only consider the phase term which is represented as :

$$\Delta\phi(t, d, \tau) = \phi(t) - \phi(t - d) - \phi(t + \tau) + \phi(t - d + \tau). \quad (17)$$

If $\Delta\phi(t, d, \tau)$ depends only on d and τ , we can say $i_{AC}(t)$ is stationary.

3.1 Necessary Condition

Here, we aim to find the conditions under which $i_{AC}(t)$ becomes stationary. We expand each term in a Taylor series around t :

$$\phi(t - d) = \phi(t) - \phi'(t)d + \frac{\phi''(t)}{2!}d^2 - \frac{\phi'''(t)}{3!}d^3 + \dots, \quad (18)$$

$$\phi(t + \tau) = \phi(t) + \phi'(t)\tau + \frac{\phi''(t)}{2!}\tau^2 + \frac{\phi'''(t)}{3!}\tau^3 + \dots, \quad (19)$$

$$\phi(t - d + \tau) = \phi(t) + \phi'(t)(\tau - d) + \frac{\phi''(t)}{2!}(\tau - d)^2 \quad (20)$$

$$+ \frac{\phi'''(t)}{3!}(\tau - d)^3 + \dots \quad (21)$$

Replacing above terms in to Eq. (17), we have

$$\Delta\phi(t, d, \tau) = \phi(t) - \phi(t - d) - \phi(t + \tau) + \phi(t - d + \tau) \quad (22)$$

$$= \frac{\phi''(t)}{2!} \{(\tau - d)^2 - \tau^2 - d^2\} + \dots \quad (23)$$

In order to make $\Delta\phi(t, d, \tau)$ non-dependent on t , $\phi''(t)$ should be constant. This indicates that $\phi(t)$ should be quadratic to make i_{AC} stationary.

3.2 Sufficiency Condition

Now, we prove all quadratic $\phi(t)$ makes $i_{AC}(t)$ stationary. Let $\phi(t) = at^2 + bt + c$. Compute each term:

$$\phi(t) = at^2 + bt + c, \quad (24)$$

$$\phi(t - d) = at^2 - 2atd + ad^2 + bt - bd + c, \quad (25)$$

$$\phi(t + \tau) = at^2 + 2at\tau + a\tau^2 + bt + b\tau + c, \quad (26)$$

$$\phi(t - d + \tau) = at^2 + 2at(\tau - d) + a(\tau - d)^2 + bt + b(\tau - d) + c \quad (27)$$

After simplifications we have:

$$\Delta\phi(t, d, \tau) = 2ad\tau, \quad (28)$$

which is t independent.

If we also consider Doppler effect, we replace b for d dependent terms to b'

$$\phi(t-d) = at^2 - 2atd + ad^2 + b't - b'd + c, \quad (29)$$

$$\phi(t-d+\tau) = at^2 + 2at(\tau-d) + a(\tau-d)^2 + b't + b'(\tau-d) + c \quad (30)$$

After simplifications we have:

$$\Delta\phi(t, d, \tau) = 2ad\tau + (b' - b)\tau, \quad (31)$$

which is still t independent.

From the above proofs for necessity and sufficiency, we can conclude that if and only if condition that makes $i_{AC}(t)$ stationary is $\phi_{LO}(t)$ to be quadratic.

4 MISCELLANEOUS DETAILS

4.1 Optical Homodyne Detection

While our primary focus is on heterodyne detection, we also examine the spectral density of homodyne detection, which involves detection without a local oscillator. In this case, the photocurrent is equivalent to that of direct detection, but we measure its spectral properties. We skip the details here, but we can derive a similar equation to that of OHD as :

$$S_i(\omega) = \eta_h' \mathcal{A}_{det}^2 S_s(\omega) * S_s^*(-\omega). \quad (32)$$

This indicates that the PSD of the photocurrent is equivalent to the autocorrelation of the optical PSD. Since $S_s(\omega)$ is a frequency-shifted version of $S_{AC}(\omega)$, the PSD $S_i(\omega)$ can be readily evaluated by taking the autocorrelation of OHD path integral.

4.2 Simulating Shot Noise

Finally, it is worth noting the simulation of shot noise, which is the primary noise source in OHD and arises from the photocurrent generated by the strong LO field. Assuming K independent photons are observed during the measurement, the photocurrent from the LO field, i_{LO} , can be expressed as:

$$i_{LO}(t) = \sum_{k=1}^K q\delta(t - t_k), \quad (33)$$

where t_k represents the arrival time of the k -th photon. Taking the Fourier transform gives

$$\tilde{i}_{LO}(\omega) = \mathcal{F}(i_{LO}(t)) = \sum_{k=1}^K qe^{-j\omega t_k}. \quad (34)$$

The PSD of the shot noise can then be calculated as:

$$S_{shot}(\omega) = \langle |\tilde{i}_{LO}(\omega)|^2 \rangle = \sum_{k=1}^K q^2 = 2qi_{LO}. \quad (35)$$

as cross-terms vanish since t_k are uncorrelated. We can also evaluate the distribution of the shot noise. Since $i_{LO}(t)$ is strong enough, a large number of photons contribute to $\tilde{i}_{LO}(\omega)$. From the central limit theorem, the real and imaginary parts of $\tilde{i}_{LO}(\omega)$ follow a Gaussian distribution, similar to speckle. Thus, the noise can be described as a complex circular Gaussian random variable, and its statistics are identical to those of the signal. To simulate the noise, one simply

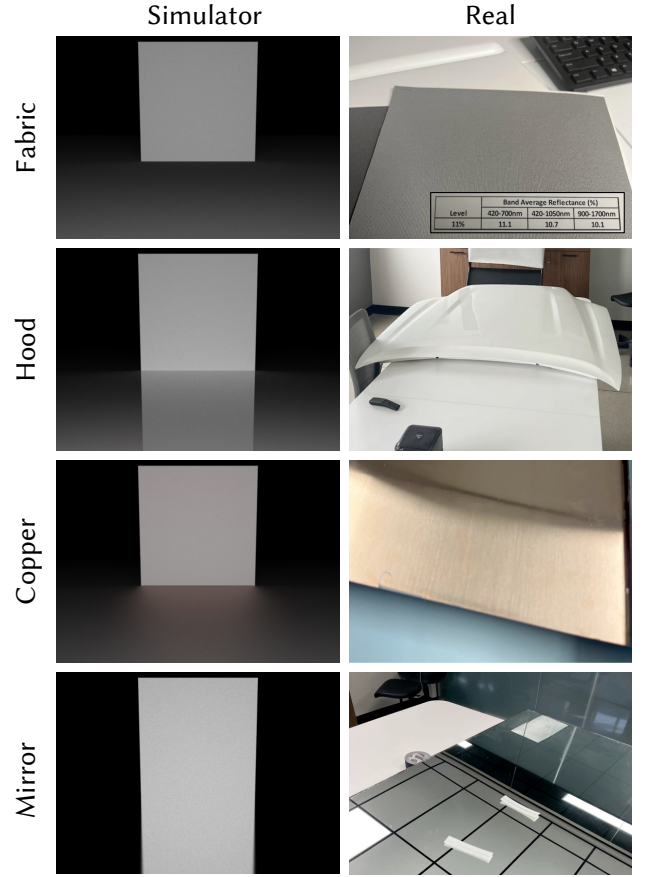


Fig. 2. Images of different materials used for both simulation and real experiment in the main manuscript.

needs to sample from a negative exponential distribution with a mean given by Eq. (35).

5 EXPERIMENTAL SETTING DETAILS

In this section, we show some details of the real-data experiment. In Fig. 2, we show different materials used in both simulation and real experiments and their simulator registration. Except for Fabric whose reflectance was directly available from the manufacturer, we rely on qualitative comparison to register the material. We tried to match the object material as closely as the real material using the Mitsuba renderer, which is listed below.

- Fabric: diffuse material with 0.1 reflectance (this is available from the manufacturer)
- Hood: coated aluminum with some roughness ($\alpha = 0.6$)
- Copper: copper with some roughness ($\alpha = 0.3$)
- Mirror: default conductor with very low roughness ($\alpha = 0.01$)
- Back Wall (Spectralon): diffuse material with 1.0 reflectance

FMCW constants for real-experiment are $B = 1$ GHz, $T = 5$ μ s, $\lambda = 1550$ nm and $M = 3072$.

REFERENCES

- Herman Z Cummins and Harry L Swinney. 1970. III light beating spectroscopy. In *Progress in optics*. Vol. 8. Elsevier, 133–200.
- David L Fried. 1967. Optical heterodyne detection of an atmospherically distorted signal wave front. *Proc. IEEE* 55, 1 (1967), 57–77.
- Joseph W Goodman. 2007. *Speckle phenomena in optics: theory and applications*. Roberts and Company Publishers.
- Shlomi Steinberg and Ling-Qi Yan. 2021. Physical Light-Matter Interaction in Hermite-Gauss Space. 40, 6 (Dec. 2021). <https://doi.org/10/gsmm8w>
- HT Yura. 1974. Optical heterodyne signal power obtained from finite sized sources of radiation. *Applied Optics* 13, 1 (1974), 150–157.